The 9th European Congress on Computational Methods in Applied Sciences and Engineering
ECCOMAS Congress 2024
3–7 June 2024, Lisboa, Portugal

NON-INTRUSIVE PHYSICAL PARAMETER INFERENCE FOR A HYPERELASTIC SOFT ROBOT SEGMENT

MINKE W. BERGHUIS[1*], ANDJELKA STANIĆ[1], ALI SADEGHI[2] AND BOJANA V. ROSIĆ[1]

[1] Applied Mechanics and Data Analysis
[2] Biomechanical Engineering
Faculty of Engineering Technology
University of Twente, Enschede
m.w.berghuis@utwente.nl

Key words: Bayesian estimation, Finite Element Analysis, hierarchical Kalman filter, inverse problem, soft robotics, soft actuators

Summary. This work proposes a hierarchical Bayesian parameter estimation framework for a nonlinear finite element model (FEM) of a hyperelastic soft pneumatic fiber reinforced actuator (FRA). The continuous fiber reinforcements are modelled as nearly inextensible truss elements embedded into an incompressible Neo-Hookean solid mesh. The Bayesian approach sequentially assimilates prior knowledge on the material constitutive behaviour with full field experimental data to obtain a posterior on the material model parameters. To avoid intrusive restarting of the FE solver at each assimilation step, both the model parameters as the model states are estimated with a discretized hierarchical linear Gauss-Markov-Kalman filter.

1 NONLINEAR PARAMETER ESTIMATION WITH FULL FIELD MEASUREMENTS

Soft continuum arms made from hyperelastic material have considerable potential in handling delicate objects and tissues, for example in clinical applications and agriculture (1; 2). The predictive modelling of soft continuum arm behaviour under quasi-static/dynamic conditions is often based on merging finite element (FE) models coming from the physics-based principles with experimental data. To deduce the underlying model parameters from observed data, one has to solve the corresponding high-dimensional inverse problem. In this paper we pose the parameter estimation problem in a probabilistic setting seen from a Bayesian point of view (3). The model parameters are assumed to be unknown and further modelled as uncertain by use of the prior experts information. Posteriors on the parameter are obtained by introducing full field displacement observations, obtained by e.g. Digital Image Correlation (4). However, this process of estimating the parameter posterior distribution usign a FE model is computationally expensive. Therefore, in this paper we propose the approximate Bayesian learning in a Kalman filter setting (5).

To make the estimation online, we pose the inference problem in a sequential manner. The current knowledge on the parameter set is updated incrementally with every new observation for each loading step. Although computationally efficient, the proposed approach requires the so-called restarting procedure of the FEM model at each increment. This means that the complete material state predicted with the previous distribution has to be rewritten with the new material state that corresponds to the current distribution. The restarting process thus can become practically cumbersome, and in some commercial FEM environments even impossible.

To address this problem we suggest the novel approach of estimating the approximate posterior distribution by using a hierarchical approach, following (6). We develop a hierarchical generalized Kalman filter approach that can be used for nonlinear problems as well as non-Gaussian parameter description (5). The hierarchical algorithm distinguishes between a master and a slave filter. The former is responsible for the parameter estimation given observation data, whereas the second is responsible for the real-time estimation of the prediction of the material state given updated parameter distribution. In this manner we achieve the restart-free estimation. The novel approach is studied with respect to the accuracy of the mean estimates on a simple example of one soft segment exposed to quasi-static loading conditions, using a Monte Carlo sampling approach (Ensemble Kalman filter (7)).

2 MODEL DEFINITION

A reinforced inflatable body that occupies region $\mathcal{G}_0$ in the reference configuration is illustrated in Fig. (1). The shaded region depicts the solid material, whereas the crosslinked lines represent the continuous reinforcement fiber, wrapped around the inflatable chamber. The body consists of a collection of material particles with initial positions $\mathbf{X}$ (see (8)). The trajectory of the particles is described by the current position $\mathbf{x}(\mathbf{X},t) = \mathbf{X} + \mathbf{u}(\mathbf{X},t)$, where $\mathbf{u}(\mathbf{X},t)$ denotes the displacement field. The local deformation is measured by the deformation gradient $\mathbf{F} = \frac{\partial \mathbf{x}}{\partial \mathbf{X}} = \nabla_0 \mathbf{x} = \mathbf{I} + \nabla_0 \mathbf{u}$. As hyperelastic material and slender structures may experience large deformation and kinematic motions, the appropriate and convenient measure of strain is the Green Lagrange strain $\mathbf{E} = \frac{1}{2}(\mathbf{C} - \mathbf{I})$ with $\mathbf{C} = \mathbf{F}^T \cdot \mathbf{F}$ being the right Cauchy Green deformation tensor and $\mathbf{S} = J\mathbf{F}^{-1} \cdot \boldsymbol{\sigma} \cdot \mathbf{F}^{-T}$ being the work conjugate second Piola Kirchhoff stress

expressed in terms of the Cauchy stress $\boldsymbol{\sigma}$ (9; 10).

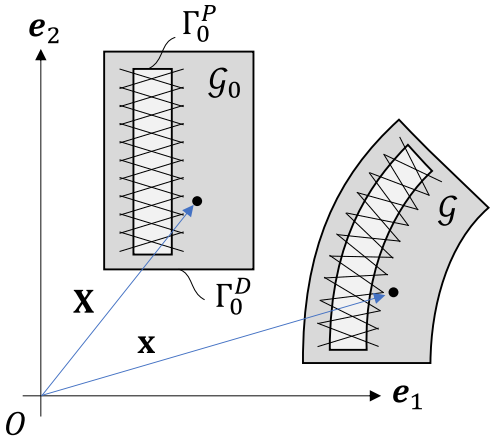

Figure 1: Deformation of a reinforced inflatable body in reference configuration $\mathcal{G}_0$ onto current configuration $\mathcal{G}$ with Dirichlet boundary Γ_0^D and pressure boundary Γ_0^D

For many elastic materials, the constitutive behaviour is described by an explicit strain energy density function. There are several particular forms of this potential, but this work considers the simple isotropic Neo-Hookean form (11; 12; 13) for the solid body:

$$\psi_{NH} = C_{10}\left(\bar{I}_1 - 3\right) + \frac{1}{D_1}\left(J-1\right)^2 \tag{1}$$

where $2C_{10} = \mu_0$ and $k_0 = \frac{2}{D_1}$ with μ_0 and k_0 being the initial shear and bulk modulus, respectively and $\bar{I}_1$ the first invariant of the isochoric right Cauchy Green deformation tensor $\bar{\mathbf{C}} = J^{-2/3}\mathbf{C}$. The dependence of ψ on the second invariant is omitted in the Neo Hookena formulation, as the sensitivity to this invariant is generally very small. Time dependence and hysteretic effects (14) are also neglected. Additionally, we assume the material to be incompressible, i.e. $D_1 \to 0$. The reinforcement fibers are assumed to be nearly inextensible and their material behaviour is described by an isotropic and homogeneous Hookean material law, as usual defined by Youngs modulus E and poisson ratio ν. The constitutive behaviour of the reinforced soft segment is thus parametrized by the set of parameters $\kappa := \{C_{10}, D_1, E, \nu\}, \kappa \in \mathbb{R}^{d_\kappa}$.

Following the previous material assumptions, the mechanical behaviour of the body can be described by the equilibrium equations, given in reference configuration by

$$\begin{aligned} \nabla_0 \cdot \mathbf{P} + \mathbf{b}_0 = \mathbf{0} \quad &\text{in} \quad \mathcal{G}_0 \\ \mathbf{u} = \mathbf{u}_0 \quad &\text{on} \quad \Gamma_0^D \\ \mathbf{P}\cdot\mathbf{N} = \mathbf{t}_N = PJ\mathbf{F}^{-T}\mathbf{N} \quad &\text{on} \quad \Gamma_0^P \end{aligned} \tag{2}$$

where $\mathbf{P} = \mathbf{FS}$ is the first Piola Kirchhoff stress, $\mathbf{b}_0 = J\mathbf{b}$ is the body force per unit undeformed volume and $\mathbf{t}_N = \frac{da}{dA}\mathbf{t}_n = |J\mathbf{F}^{-T}\mathbf{N}|\mathbf{t}_n$ (Nanson's formula) is the traction force expressed on the reference surface with normal $\mathbf{N}$, with $\mathbf{t}_n$ its counterpart on the current surface. The applied pressure with magnitude P and Dirichlet condition are imposed on their respective boundaries Γ_0^P and Γ_0^D, where $\Gamma_0^P \cap \Gamma_0^D = \emptyset$, see Fig. (1).

The weak form of Eq. (2) is spatially discretized using the Finite Element Method (15; 16; 8). The displacement field of the solid body is approximated by 20-node (i.e. serendipity) quadratic brick elements, using reduced integration. The incompressibility condition is enforced by augmenting the displacement field with an indepedent hydrostatic pressure field leading to the mixed formulation (17; 18; 16). The pressure stress is discretized independently, introducing additional degrees of freedom to these hybrid elements. The pressure is assumed to be linear in second order elements. This approach simultaneously avoids volumetric locking effects, at the cost of additional pressure variables that act as Lagrange multipliers (19; 15). The reinforcements are discretized using 3-node quadratic truss elements. These elements are embedded into the solid elements using the 'embedded element' constraint following (20; 21), see also (22) for a short history of developments. Benefits of this formulation are the independent meshing of the host and reinforcement fibers without the introduction of additional degrees of freedom. For the sake of simplicity, it is assumed that the fibers adhere perfectly to the solid mesh, i.e. there is a no slip bond, as the configuration of the fibers does not lead to pull-out behaviour. The two non-conforming meshes are then coupled by imposing the relevant kinematic coupling constraints. The translational degrees of freedom of the embedded nodes are constrained to the interpolated values of the host element. This embedding formulation therefore modifies the stiffness matrix of the host elements, see (23). It is clear that due to the geometrical component this modified stiffness matrix need not be symmetrical.

The nonlinear static equilibrium equations for the incompressible hyperelastic material with embedded trusses is solved using the full Newton method (8; 24; 16). This method has high accuracy and fast (quadratic) convergence, compared to the alternate modified- and quasi-Newton methods.

3 BAYESIAN PARAMETER ESTIMATION

The finite element problem posed in the previous section can be solved for the model state x in $\mathbb{R}^{d_x}$ given the parameter set κ, that is usually unknown before collecting experimental data. The model state for a dynamic finite element analysis with mixed formulation includes the nodal displacements, velocities and hydrostatic pressure variables. Experimental observations provide indirect information on κ and thus κ can only be estimated. In this paper we assume that κ is a priori unknown and thus uncertain. Hence, we employ the probabilistic formulation of the aforementioned inverse problem.

Let $F : \mathbb{R}^{d_x} \times \mathbb{R}^{d_\kappa} \times \mathbb{R}^+ \to \mathbb{R}^k$ be a function describing the nonlinear evolution of the full model state of the body according to:

$$\dot{x}(t) = F(x(\kappa), \kappa, t) + \epsilon(t), \quad \kappa \in \mathbb{R}^{d_\kappa}, \quad x \in \mathbb{R}^{d_x}, \quad x(0) = x_0 \in \mathbb{R}^{d_x}. \tag{3}$$

The previous equation describes the abstract formulation of the semi-discretized finite element problem stated in section 2. The following estimation approach can also be applied on applications more general than the soft reinforced segment.

The state given in Eq. (3) can only be partially observed following:

$$z(t) = y(t) + \varepsilon(t), \quad y(t) = H(x(t), \kappa, t), \quad z(t) \in \mathbb{R}^{d_z} \tag{4}$$

in which $H : \mathbb{R}^{d_x} \times \mathbb{R}^{d_\kappa} \times \mathbb{R}^+ \to \mathbb{R}^{d_z}$ is a possibly nonlinear function and y denotes the noiseless model signal. The goal is to estimate κ by having the finite data set

$$\mathbb{R}^{d_z} \ni z_k = H(\hat{x}(t_k), \hat{\kappa}, t_k) + \hat{\varepsilon}_k, \quad k = 1, ..., N \tag{5}$$

at equidistant sample times t_k in a predefined time interval $k = 1, ..., N$, where the quantities with $\hat{}$ represent the "true" values of the model state, parameters and observation noise. The modeling- $\epsilon_k := \epsilon(t_k)$ and observation noise $\varepsilon_k := \varepsilon(t_k)$ are assumed to be additive and i.i.d. sequences.

This work adopts a Bayesian approach to estimation by the help of which the lack of knowledge on κ, i.e. the "extended state" $q := (x_0, \kappa)$, can be modelled a priori as a random variable (RV) $q(\omega_q) \in L_2(\Omega_q, \mathfrak{F}_q, \mathbb{P}_q)$ assumed to be independent from the measurement and modeling noise ε_k and ϵ_k at time instances $t_k, k = 0, ..., k_T$, respectively [1]. Given the whole history of observations $z_{1:N} = [z_k]_{k=1}^N$ and the prior probability density function $p(q)$, one may estimate the posterior of the extended state $p(q|z_{1:N})$ by use of Bayes´ rule

$$p(q|z_{1:N}) = \frac{p(z_{1:N}|q)p(q)}{p(z_{1:N})}, \tag{6}$$

in which $p(z_{1:N}|q)$ denotes the corresponding likelihood function defined by the shape of the measurement noise. It is clear that in this general formulation, the prior parameter uncertainty $p(q)$ has to be propagated through the evolution and observation model given in Eq. (3) and Eq. (4), respectively, over the whole time interval $[0, T]$. The previously described estimation is performed only once after collection of all measurement data. See Fig. (2a), for a schematic representation of this general update, where the state evolves along the horizontal axis. State uncertainty is depicted by the shaded regions, that represent the lower and upper (e.g. the 10th and 90th) percentiles of the distribution. The probability density functions (pdfs) of the prior and posterior state evaluated at discrete time instances are depicted along intermediate vertical axes. The general estimation is of an offline type and thus cannot be used in real time measurements. Therefore, in this paper the previous problem is restated as a sequential estimation problem as described hereafter.

3.1 Sequential Gauss-Markov-Kalman filter

Assuming that the state evolution is a one step Markov process, one may introduce the prior, i.e. forecast, $p(q_{k,f}) := p(q_k|z_{1:k-1})$ describing the extended state at time t_k as

$$p(q_{k,f}) = p(q_k|q_{k-1})p(q_{k-1}|z_{1:k-1}) = p(q_k|q_{k-1})p(q_{k-1,a}), \tag{7}$$

where $p(q_{k-1,a}) := p(q_{k-1}|z_{1:k-1})$ denotes assimilated entity in the previous time step. Clearly, the previous posterior $p(q_{k-1,a})$ is evolved from $k-1$ to k by the evolution model given in Eq. (3) to obtain the prior for the state q_k at the current timestep, as well as likelihood function in Eq. (7). The sequential assimilation then reads as

$$p(q_{k,a}) = p(q_k|z_{1:k}) \propto p(z_k|q_k)p(q_{k,f}). \tag{8}$$

The previous equation is further referred as the *master filter*. See Fig. (2b) for a schematic representation of this filter, shaded regions and pdfs at at discrete time instances are defined as before.

[1] Note that state q_k contains both the model state x_k and the parameter set κ

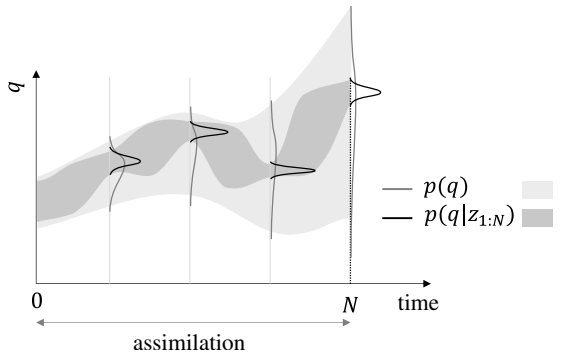

(a) General assimilation with $p(q)$ and $p(q|z_{1:N})$) the joint pdf of all priors and posteriors from Eq. (6)

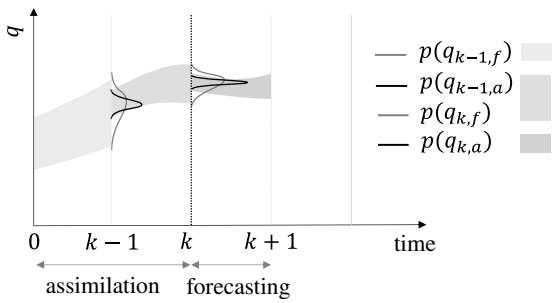

(b) Sequential filter, forecasting the state $p(q_{k,f})$ with the assimilated state $p(q_{k-1,a})$ using the evolution model

Figure 2: Schematic representation of assimilation approaches, given all observations until time instance k. Lines denote pdf at discrete time instences, regions denote the upper and lower percentiles of the continuous pdf implied by the evolution model.

As the full probability (density) in Eq. (8) is often not required in engineering practice, we first estimate only the expected value of the state given the observations. Therefore, the problem of conditional probability densities in Eq. (8) is reformulated into estimating

$$\mathbb{E}(q_k|z_k) = \int q_k p(q_k|z_k) dq_k \tag{9}$$

sequentially. The conditional expectation of a RV $q_{k,f}$ given a RV $z_{k,f}$ is a measurable function $\varphi(\cdot)$ of $z_{k,f}$ (Doob-Dynkin lemma (25)). Following (26; 5), one may then introduce the Gauss-Markov-Kalman filter

$$q_{k,a} = \varphi(z_k;\theta) + (q_{k,f} - \varphi(z_{k,f};\theta)), \tag{10}$$

with φ being the optimal map parameterized by θ. The latter can be estimated in a mean squared sense according to:

$$\theta^* = \arg\min_{\theta} \|q_{k,f} - \varphi(z_{k,f},\theta)\|^2. \tag{11}$$

The simplest possible choice for the optimal map φ is affine map:

$$\varphi(z_{k,f}) = K z_{k,f} + b, \tag{12}$$

parametrized by the Kalman gain K and the bias term b, i.e. $\theta := \{K, b\}$. By solving the corresponding optimization problem in Eq. (11) and assuming the observation model in Eq. (4) one obtains

$$K = \Sigma_{q_{k,f} y_{k,f}} (\Sigma_{y_{k,f}} + \Sigma_{\varepsilon_{k,f}})^{-1}, \tag{13}$$

where

$$\Sigma_{q_{k,f} y_{k,f}} := \mathbb{E}\left((q_{k,f} - \mathbb{E}(q_{k,f}))(y_{k,f} - \mathbb{E}(y_{k,f}))\right)$$

is the cross covariance matrix between $q_{k,f}$ and $y_{k,f}$ with $\Sigma_{y_{k,f}}$ and $\Sigma_{\varepsilon_{k,f}}$ being the covariance matrices of the forecasted observation and observation noise. Following this, the sequential update in Eq. (8) becomes

$$q_{k,a} = q_{k,f} + K(z_k - z_{k,f}). \tag{14}$$

In a Gaussian case this is equivalent to the classical Kalman filter estimate (i.e. MAP) (27). The previous formulation Eq. (14) describes the estimation of the expected value of Eq. (8).

3.2 Hierarchical estimation

The sequential forecasted state presents a problem for large FE models, as the evolution model (time integration) has to be evaluated using the updated state $q_{k,a}$ to predict $p(q_{k+1,f})$. For a finite element procedure this means that both the model state x_k and the parameters κ have to be exported from the FE solver at time step t_k, assimilated externally using Eq. (14) and then imported back into the FE software. After this, the integration can be continued until the prediction time t_{k+1}. For large state models, this poses memory problems. Alternatively, one could restart the time integration from t_0 with the updated parameters and initial conditions (restarting approach) after each assimilation step. In contrast to the memory problem, this may lead to very long computational times that are not suited for the use in practice.

This work proposes to consider the forecasting step as an estimation problem too, following (6), by exploiting the Markovian property of the states. The idea is to introduce master and slave filters in which the former plays a role of assimilating real measurement data into the system following Eq. (14), whereas the latter has to take care of the prediction step needed for estimating the forecasted observation $z_{k,f}$. To achieve this, we propose to offline perform the uncertainty quantification of the observation z_k given given the initial prior $p(q_{0,f}) := p(x_{0,f}, \kappa_{0,f})$ over the complete time interval $[0, T]$ to obtain:

$$y_{k,fe} = H(x_{k,fe}, \kappa_{0,f}, t_k) \quad k = 1, ..., N \tag{15}$$

in which the subscript fe stands for the forecast of the observation that is not the same as the forecast of the observation given in Eq. (14). The main difference is that the state $y_{k,fe}$ in Eq. (15) is calculated given *initial prior* $p(x_{0,f})$ of the state and the parameter $p(\kappa_{0,f})$ at time t_0, whereas the forecast of the observation used in Eq. (14) is calculated given the *current prior* $p(q_{k,f})$ at the time t_k such that:

$$y_{k,f} = H(x_{k,f}, \kappa_{k,f}, t_k) \tag{16}$$

and

$$z_{k,f} = y_{k,f} + \varepsilon_k \tag{17}$$

hold. As we need the latter and not the former, we use the assumption that the next prior on the parameter set $p(\kappa_{k+1,f})$, falls under (i.e. is narrower than) the initial prior $p(\kappa_{0,f})$ reflecting the arrival of the new measurement information in the assimilation process. For a constant parameter, the next parameter prior is simply the current parameter posterior in Eq. (14), i.e. $p(\kappa_{k+1,f}) = p(\kappa_{k,a})$, see Eq. (7). Hence, we can use this information from the current time instance to estimate the state $y_{k+1,f}$ given the state $y_{k+1,fe}$ and the pair $p(\kappa_{0,f})$ and $p(\kappa_{k,a})$. For this we can use another linear Kalman filter, further referred as a slave filter, that reads:

$$y_{k+1,ae} = y_{k+1,fe} + B(\kappa_{k,a} - (\kappa_{0,f} + e_k)) \tag{18}$$

in which $p(y_{k+1,ae})$ denotes the posterior estimate of $p(y_{k+1,f}|z_{1:k})$. The pseudo-measurement of the assimilated parameter is denoted $\kappa_{k,a}$ and $y_{k+1,fe}$ is the pseudo-prior $p(y_{k+1,f}|z_{1:k-1})$. We introduce the pseudo-measurement error e_k following (6). See Fig. (**??**) for a schematic representation of the slave filter, where the offline uncertainty quantification of the state is denoted with the shaded region as before, and the current observation prediction is estimated using this forecasted evolution, i.e. without time integration of the evolution model. The master filter in Eq. (14) with the slave filter estimate of the current observation in Eq. (18) and Eq. (17) is thus

$$q_{k,a} = q_{k,f} + K\left(z_k - (y_{k,ae} + \varepsilon_k)\right). \tag{19}$$

After this state assimilation with the master filter, the slave filter estimates the observation forecast for the next time step, and the process is repeated each time an observation becomes available for assimilation.

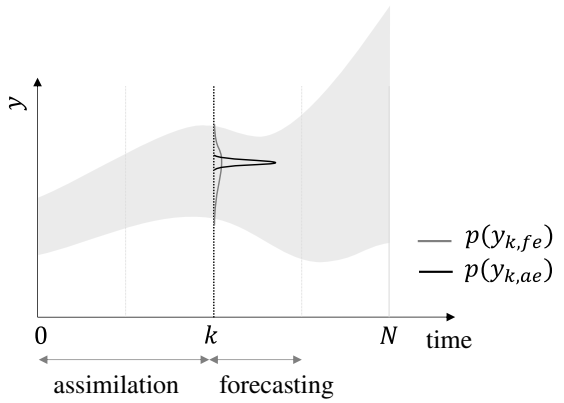

Figure 3: Hierarchical assimilation, given all observations until time instance k with predictions until N. Lines denote pdf at discrete time, regions denote the continuous pdf implied by the evolution model.

3.3 Ensemble based hierarchical Gauss-Markov-Kalman filter

In this paper we exploit a Monte Carlo approach to discretize Eq. (14) and Eq. (18) and propagate an ensemble of N_s draws from the prior $q_{0,f}(n)$ through the model to obtain an ensemble of N_s predicted observations and use these to assimilate the parameter posterior (28; 29). The state ensemble at time index k is denoted by $\mathbf{Q}_k := [q_k(\omega_1), ..., q_k(\omega_n)]$ and the predicted observation ensemble by $\mathbf{Y}_k := [y_k(\omega_1), ..., y_k(\omega_n)]$, where subscripts $_{f,a}$ are added to denote the assimilated and forecasted ensembles and $_{fe,ae}$ the assimilated and forcasted evolution ensembles (6). The observation forecast is perturbed with an ensemble of samples from the assumed noise model $\varepsilon_k \sim \mathcal{N}(0, R_k)$ denoted $\mathbf{E}_k := [\varepsilon_k(\omega_1), ..., \varepsilon_k(\omega_n)]$. This pertubation of the signal with the assumed noise model is needed to avoid underestimation of the assimilated error covariance matrix with updating each ensemble member with the same Kalman update, see (30; 31; 32). The expected value of the state

$$\mathbb{E}(q_k) = \int q_k \mathbb{P}(d\omega) \tag{20}$$

is estimated by the sample mean

$$\bar{q}_k := \frac{1}{N_s} \sum_{n=1}^{N_s} q_k(\omega_n)$$

in which $q_k(\omega_n)$ is a sequence of i.i.d. random variables.

The covariances in the (pseudo-) Kalman gain in Eq. (14) and Eq. (18) are approximated by the sample covariances of the ensembles (7; 33)

$$\Sigma_{q_k y_k} \approx C_{q_k y_k} := \frac{1}{N_s - 1} \sum_{n=1}^{N_s} (q_k(\omega_n) - \bar{q}_k)(y_k(\omega_n) - \bar{y}_k)^T$$

$$\Sigma_{y_k} \approx C_{y_k} := \frac{1}{N_s - 1} \sum_{n=1}^{N_s} (y_k(\omega_n) - \bar{y}_k)(y_k(\omega_n) - \bar{y}_k)^T$$

and

$$\Sigma_{y_k q_k} \approx C_{y_k q_k} := \frac{1}{N_s - 1} \sum_{n=1}^{N_s} (y_k(\omega_n) - \bar{y}_k)(q_k(\omega_n) - \bar{q}_k)^T$$

$$\Sigma_{q_k} \approx C_{q_k} := \frac{1}{N_s - 1} \sum_{n=1}^{N_s} (q_k(\omega_n) - \bar{q}_k)(q_k(\omega_n) - \bar{q}_k)^T$$

These sample covariances are interpreted as the sensitivity of the state to observation model Eq. (4), evaluated around the sample mean (34; 35; 36). Both the finite number of samples as the possible model nonlinearity distinguish the sample covariance from the covariance (37).

3.4 Hierarchical sequential EnKF

The sequential assimilation with hierarchical update can be summarized as follows. First, the prior state ensemble $\mathbf{Q}_{0,f}$ is propagated through the (nonlinear) forward model to obtain the forecasted signal evolutions $\mathbf{Y}_{k,fe}$ in Eq. (15). Second, at each assimilation timestep k, both the state and the observation forecasts are assimilated with the available observations. The state update is then given by the master filter, see Eq. (14),

$$\mathbf{Q}_{k,a} = \mathbf{Q}_{k,f} + \mathbf{K}_k(\mathbf{z}_k - (\mathbf{Y}_{k,ae} + \mathbf{E}_k)), \tag{21}$$

where $\mathbf{z}_k$ are the collected observations at the current timestep and the Kalman gain is computed as

$$\mathbf{K}_k = C_{q_k,y_k}(C_{y_k,y_k} + R_{z,k})^{-1}.$$

The state forecast for the next timestep is given by

$$\mathbf{Q}_{k+1,f} = \mathbf{Q}_{k,a} \tag{22}$$

and the signal evolution forcast for the next timestep is updated by the slave filter

$$\mathbf{Y}_{k+1,ae} = \mathbf{Y}_{k+1,fe} + \mathbf{B}_k(\mathbf{Q}_{k,a} - (\mathbf{Q}_{0,f} + \mathbf{E}_{q,k})), \tag{23}$$

where the indices are defined as before and the pseudo Kalman gain is computed by

$$\mathbf{B}_k = C_{y_k,q_k}(C_{q_k,q_k} + R_{q,k})^{-1},$$

in which the state pertubation covariance matrix $R_{q,k}$ is introduced following (6) to account for the transformed observation error in the assimilated state.

4 NUMERICAL RESULTS

A finite element model is made for a soft inflatable segment with initially square cross section of dimension $16\times16\times60$ mm^3 see Fig. (4). The soft body has a hollow cylindrical cavity of radius 2 mm, located 5 mm from the segment centroidal axis. The cavity is closed off with 10 mm thick endcaps and reinforced with 0.1 mm diameter fibers, that are wrapped with a radius of 3 mm around the cavity center in a double helix pattern with a 2° pitch angle. The solid body is

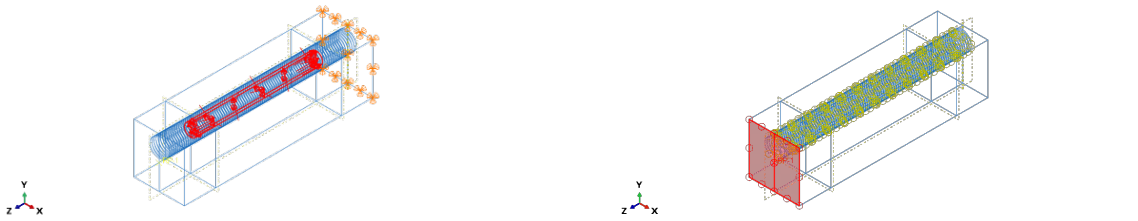

(a) Boundary conditions (clamped-free) and pressure load

(b) rigid top surface and embedded fiber constraints

Figure 4: Schematic FEM

partitioned such that a structured mesh of solid hybrid quadratic brick elements with reduced integration (Abaqus; C3D20RH) is possible. The reinforcement fibers are meshed into quadratic truss elements (Abaqus: T3D3) and embedded into the solid mesh with the previously described embedding constraint. The segment top surface is constrained to remain flat and undeformed, as the fabricated segment also has a solid endcap, see Fig. (4b). The bottom end of the segment is considered clamped. A pressure load of 0.022 MPa is applied incrementally to the hollow chamber, see Fig. (4a), matching the pressure magnitude of the experiments.

The fiber material is modelled as an axially stiff Hookean material (cotton fiber) with Youngś modulus 31 GPa and Poisson ratio 0.36. The soft hyperelastic material is modelled as an incompressible Neo-Hookean solid with unknown material parameter C_{10}. As this parameter has to be positive definite based on physical grounds, we model it a priori as a lognormal RV $C_{10} \sim log\mathcal{N}\left(1.1\kappa_t, (0.2\kappa_t)^2\right)$ with $\kappa_t = 0.005615MPa$. For the ensemble representation we use $N_s = 100$ Monte Carlo samples.

The nodes that are observed are on the front $y-z$ surface of the segment, as only this surface is in line of sight of the experimental camera. Only y and z displacements are observed, as the out of plane displacements cannot be directly captured and have a too low signal-to-noise ratio.

The FEM output is synchronized by linear interpolation to the measurement sample rate such that observations are predicted for each $\Delta t = 0.01$ on a normalized timescale $0 \leq t \leq 1$.

4.1 Perturbed FEM numerical experiment

The assimilation approach is demonstrated first on a numerical experiment with known model parameter $C_{10} = 0.0048MPa$, which is in a region of low probability in the chosen prior. The observations are the perturbed values of the true model output. The observation noise is assumed to be independent for each node with $\varepsilon_k \sim \mathcal{N}\left(0, 1^2\right)$. State perturbation is set to zero $\varepsilon_{q,k} \sim \mathcal{N}\left(0, 0^2\right)$. Assimilation results of the sequential hierachical filter in Eq. (21) and Eq. (23) over (quasi) time are plotted in Fig. (5a). The states and observations evolve along the

horizontal axis. The shaded regions show the $10-90\%$ percentiles, whereas the markers show the deterministic value or the sample mean of the plotted quantity. For plotting purposes, only a single observed node is plotted, i.e. a top center node at initial location of $(y, z) = (0.0, 40.0)$ mm, alongside the state q, which in this case only holds the unknown parameter C_{10}. In Fig. (5b) the pdfs of the prior (solid red line) at t_0 and posterior (dashed green line) at $t = 1$ are plotted along with the known 'true' value of the parameter (vertical solid black line). It is clear that the posterior has reduced variance and the sample approximation of the sample mean finds the true parameter value.

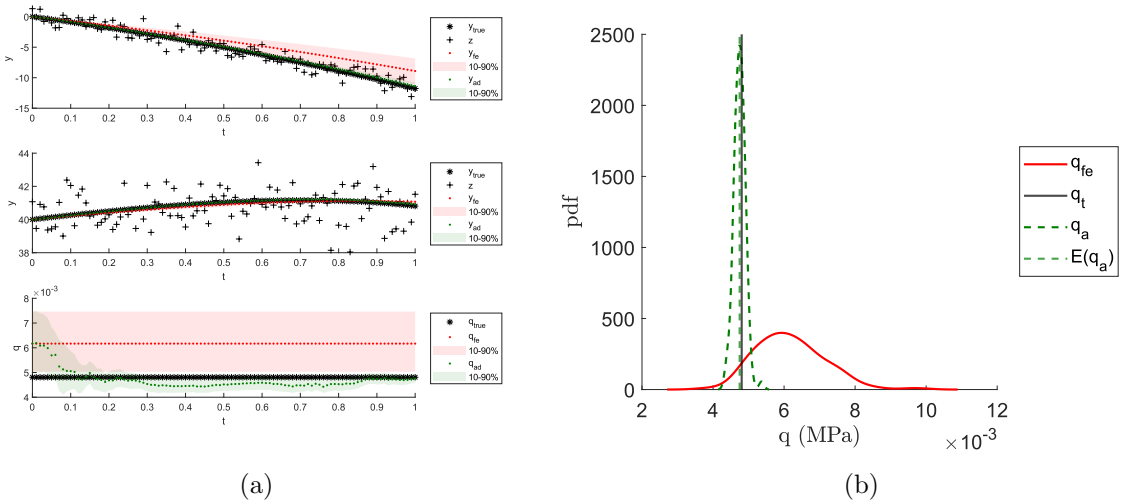

(a) (b)

Figure 5: Perturbed FEM experiment

5 CONCLUSION

In this work we propose a hierarchical linear Gauss-Markov-Kalman filter for parameter estimation using a nonlinear FEM model and full field observations. The master filter assimilates the prior parameter knowledge with the information from the experimental data. The slave filter avoids the sequential restart of the FEM model by also estimating the observation predictions. The approach is demonstrated on a FE model of a hyperelastic soft pneumatic fiber reinforced actuator. The continuous nearly inextensible fiber reinforcements are embedded into the incompressible Neo-Hookean solid mesh. It is shown that the hierarchical filter reduces the parameter uncertainty within the span of the experiment and finds the known true parameter value for a perturbed numerical experiment.

References

[1] D. Trivedi, C. D. Rahn, W. M. Kier, and I. D. Walker, "Soft robotics: Biological inspiration, state of the art, and future research," *Applied bionics and biomechanics*, vol. 5, no. 3, pp. 99–117, 2008.

[2] O. Yasa, Y. Toshimitsu, M. Y. Michelis, L. S. Jones, M. Filippi, T. Buchner, and R. K. Katzschmann, "An overview of soft robotics," *Annual Review of Control, Robotics, and Autonomous Systems*, vol. 6, no. 1, pp. 1–29, 2023.

[3] B. V. Rosić, A. Litvinenko, O. Pajonk, and H. G. Matthies, "Sampling-free linear bayesian update of polynomial chaos representations," *Journal of Computational Physics*, vol. 231, no. 17, pp. 5761–5787, 2012.
[4] M. A. Sutton, J. J. Orteu, and H. Schreier, *Image correlation for shape, motion and deformation measurements: basic concepts, theory and applications*. Springer Science & Business Media, 2009.
[5] B. V. Rosić, A. Kučerová, J. Sỳkora, O. Pajonk, A. Litvinenko, and H. G. Matthies, "Parameter identification in a probabilistic setting," *Engineering Structures*, vol. 50, pp. 179–196, 2013.
[6] S. Dobrilla, M. Lunardelli, M. Nikolić, D. Lowke, and B. Rosić, "Bayesian inference of mesoscale mechanical properties of mortar using experimental data from a double shear test," *Computer methods in applied mechanics and engineering*, vol. 409, p. 115964, 2023.
[7] G. Evensen, "The ensemble kalman filter: Theoretical formulation and practical implementation," *Ocean dynamics*, vol. 53, pp. 343–367, 2003.
[8] K.-J. Bathe, *Finite element procedures*. Klaus-Jurgen Bathe, 1996.
[9] M. F. Beatty, "Topics in finite elasticity: hyperelasticity of rubber, elastomers, and biological tissues—with examples," 1987.
[10] J. Bonet and R. D. Wood, *Nonlinear continuum mechanics for finite element analysis*. Cambridge university press, 1997.
[11] L. G. Treloar, *The physics of rubber elasticity*. OUP Oxford, 1975.
[12] O. H. Yeoh, "Some forms of the strain energy function for rubber," *Rubber Chemistry and technology*, vol. 66, no. 5, pp. 754–771, 1993.
[13] E. M. Arruda and M. C. Boyce, "A three-dimensional constitutive model for the large stretch behavior of rubber elastic materials," *Journal of the Mechanics and Physics of Solids*, vol. 41, no. 2, pp. 389–412, 1993.
[14] J. S. Bergström and M. C. Boyce, "Constitutive modeling of the large strain time-dependent behavior of elastomers," *Journal of the Mechanics and Physics of Solids*, vol. 46, no. 5, pp. 931–954, 1998.
[15] J. T. Oden, *Finite elements of nonlinear continua*. McGraw-Hill, 1972.
[16] O. C. Zienkiewicz and R. L. Taylor, *The finite element method set*. Elsevier, 2005.
[17] J. Deteix, T. Diop, and M. Fortin, *Numerical Methods for Mixed Finite Element Problems: Applications to Incompressible Materials and Contact Problems*, vol. 2318. Springer Nature, 2022.
[18] M. Fortin and F. Brezzi, *Mixed and hybrid finite element methods*, vol. 51. New York: Springer-Verlag, 1991.
[19] L. R. Herrmann, "Elasticity equations for incompressible and nearly incompressible materials by a variational theorem.," *AIAA journal*, vol. 3, no. 10, pp. 1896–1900, 1965.
[20] Y. M. Cheng and Y. Fan, "Modeling of reinforcement in concrete and reinforcement confinement coefficient," *Finite elements in analysis and design*, vol. 13, no. 4, pp. 271–284, 1993.
[21] D. Phillips and O. Zienkiewicz, "Finite element non-linear analysis of concrete structures.," *Proceedings of the Institution of Civil Engineers*, vol. 61, no. 1, pp. 59–88, 1976.
[22] L. A. Bitencourt Jr, O. L. Manzoli, Y. T. Trindade, E. A. Rodrigues, and D. Dias-da Costa, "Modeling reinforced concrete structures using coupling finite elements for discrete representation of reinforcements," *Finite Elements in Analysis and Design*, vol. 149, pp. 32–44, 2018.
[23] H.-G. Kwak and F. Filippou, "Finite element analysis of reinforced concrete structures under monotonic loads," 1990.
[24] P. Bergan, G. Horrigmoe, B. Bråkeland, and T. Søreide, "Solution techniques for non- linear finite element problems," *International Journal for Numerical Methods in Engineering*, vol. 12, no. 11, pp. 1677–1696, 1978.
[25] A. Bobrowski, *Functional analysis for probability and stochastic processes: an introduction*. Cambridge University Press, 2005.
[26] H. G. Matthies, E. Zander, B. V. Rosić, A. Litvinenko, and O. Pajonk, "Inverse problems in a bayesian setting," *Computational Methods for Solids and Fluids: Multiscale Analysis, Probability Aspects and Model Reduction*, pp. 245–286, 2016.
[27] S. M. Kay, *Fundamentals of statistical signal processing: estimation theory*. Prentice-Hall, 1993.

[28] P. K. Kitanidis, "Quasi-linear geostatistical theory for inversing," *Water resources research*, vol. 31, no. 10, pp. 2411–2419, 1995.

[29] D. S. Oliver, N. He, and A. C. Reynolds, "Conditioning permeability fields to pressure data," in *ECMOR V-5th European conference on the mathematics of oil recovery*, pp. cp–101, European Association of Geoscientists & Engineers, 1996.

[30] J. S. Whitaker and T. M. Hamill, "Ensemble data assimilation without perturbed observations," *Monthly weather review*, vol. 130, no. 7, pp. 1913–1924, 2002.

[31] P. L. Houtekamer and H. L. Mitchell, "Data assimilation using an ensemble kalman filter technique," *Monthly weather review*, vol. 126, no. 3, pp. 796–811, 1998.

[32] G. Burgers, P. J. Van Leeuwen, and G. Evensen, "Analysis scheme in the ensemble kalman filter," *Monthly weather review*, vol. 126, no. 6, pp. 1719–1724, 1998.

[33] P. Sakov, D. S. Oliver, and L. Bertino, "An iterative enkf for strongly nonlinear systems," *Monthly Weather Review*, vol. 140, no. 6, pp. 1988–2004, 2012.

[34] Y. Chen and D. S. Oliver, "Levenberg–marquardt forms of the iterative ensemble smoother for efficient history matching and uncertainty quantification," *Computational Geosciences*, vol. 17, pp. 689–703, 2013.

[35] G. Evensen, "Accounting for model errors in iterative ensemble smoothers," *Computational Geosciences*, vol. 23, no. 4, pp. 761–775, 2019.

[36] A. C. Reynolds, M. Zafari, and G. Li, "Iterative forms of the ensemble kalman filter," in *ECMOR X-10th European conference on the mathematics of oil recovery*, pp. cp–23, European Association of Geoscientists & Engineers, 2006.

[37] G. Evensen, F. C. Vossepoel, and P. J. Van Leeuwen, *Data assimilation fundamentals: A unified formulation of the state and parameter estimation problem*. Springer Nature, 2022.